# 2-Cysteine Peroxiredoxins and Thylakoid Ascorbate Peroxidase Create a Water-Water Cycle That Is Essential to Protect the Photosynthetic Apparatus under High Light Stress Conditions[1]

**Jasmin Awad[2], Henrik U. Stotz[2,3], Agnes Fekete, Markus Krischke, Cornelia Engert, Michel Havaux, Susanne Berger, and Martin J. Mueller***

Julius-von-Sachs-Institute of Biosciences, Biocenter, Pharmaceutical Biology, University of Wuerzburg, D–97082 Wuerzburg, Germany (J.A., H.U.S., A.F., M.K., C.E., S.B., M.J.M.); and Biologie Végétale et Microbiologie Environnementales, Unité Mixte de Recherche 7265 Centre National de la Recherche Scientifique-Commissariat à l'Energie Atomique-Aix Marseille University, 13108 Saint-Paul-lez-Durance, France (M.H.)

Different peroxidases, including 2-cysteine (2-Cys) peroxiredoxins (PRXs) and thylakoid ascorbate peroxidase (tAPX), have been proposed to be involved in the water-water cycle (WWC) and hydrogen peroxide ($H_2O_2$)-mediated signaling in plastids. We generated an Arabidopsis (*Arabidopsis thaliana*) double-mutant line deficient in the two plastid 2-Cys PRXs (2-Cys PRX A and B, *2cpa 2cpb*) and a triple mutant deficient in 2-Cys PRXs and tAPX (*2cpa 2cpb tapx*). In contrast to wild-type and *tapx* single-knockout plants, *2cpa 2cpb* double-knockout plants showed an impairment of photosynthetic efficiency and became photobleached under high light (HL) growth conditions. In addition, double-mutant plants also generated elevated levels of superoxide anion radicals, $H_2O_2$, and carbonylated proteins but lacked anthocyanin accumulation under HL stress conditions. Under HL conditions, 2-Cys PRXs seem to be essential in maintaining the WWC, whereas tAPX is dispensable. By comparison, this HL-sensitive phenotype was more severe in *2cpa 2cpb tapx* triple-mutant plants, indicating that tAPX partially compensates for the loss of functional 2-Cys PRXs by mutation or inactivation by overoxidation. In response to HL, $H_2O_2$- and photooxidative stress-responsive marker genes were found to be dramatically up-regulated in *2cpa 2cpb tapx* but not *2cpa 2cpb* mutant plants, suggesting that HL-induced plastid to nucleus retrograde photooxidative stress signaling takes place after loss or inactivation of the WWC enzymes 2-Cys PRX A, 2-Cys PRX B, and tAPX.

Plants are frequently exposed to different abiotic stresses, including high light (HL), UV irradiation, heat, cold, and drought. A component common to these stresses is the rapid formation of reactive oxygen species (ROS) as the result of metabolic dysbalances. A major ROS produced under moderate light (ML) and, in particular, HL photooxidative stress conditions was shown to be singlet oxygen, $^1O_2$, that is produced in illuminated chloroplasts predominantly at the PSII (Triantaphylidès et al., 2008). Most of the singlet oxygen is quenched by carotenoids and tocopherols or reacts with galactolipids in thylakoid membranes, yielding galactolipid hydroperoxides (Zoeller et al., 2012; Farmer and Mueller, 2013). In addition, superoxide radicals, $O_2\cdot^-$, are produced predominantly at the PSI and rapidly dismutate to hydrogen peroxide ($H_2O_2$) either spontaneously or because of being catalyzed by superoxide dismutase. Hence, lipid peroxides and $H_2O_2$ are produced close to the photosystems and may damage thylakoid proteins. In this context, 2-Cys peroxiredoxin (PRX) enzymes have been implicated in the reductive detoxification of lipid peroxides and $H_2O_2$ (König et al., 2002).

During photosynthesis, light energy absorbed by PSII is used to split water molecules, and the electrons are channeled from PSII through PSI to ferredoxin (Fd). As a result, electrons flow from water to Fd. The main electron sink reaction is the Fd NADP oxidoreductase-catalyzed production of NADPH that functions as an electron donor to reduce carbon dioxide to sugars. Under HL conditions, excessive excitation energy is dissipated into heat, which was indicated by nonphotochemical quenching of chlorophyll fluorescence. In addition, excessive photosynthetic electrons can be donated from PSI to $O_2$, yielding $O_2\cdot^-$ (Miyake, 2010). This process, the Mehler reaction, creates an alternative electron sink and electron flow. Superoxide anion radicals, $O_2\cdot^-$, can be dismutated to $O_2$ and $H_2O_2$ by a thylakoid-attached copper/zinc superoxide dismutase (Cu/ZnSOD; Rizhsky et al., 2003). $H_2O_2$

[1] This work was supported by the Deutsche Forschungsgemeinschaft (grant no. GRK1342).

[2] These authors contributed equally to the article.

[3] Present address: School of Life and Medical Sciences, University of Hertfordshire, Hatfield, Hertfordshire AL10 9AB, United Kingdom.

* Address correspondence to martin.mueller@biozentrum.uni-wuerzburg.de.

The author responsible for distribution of materials integral to the findings presented in this article in accordance with the policy described in the Instructions for Authors (www.plantphysiol.org) is: Martin J. Mueller (martin.mueller@biozentrum.uni-wuerzburg.de).

www.plantphysiol.org/cgi/doi/10.1104/pp.114.255356

 

can then be reduced to water by peroxidases. As a result, $O_2$ molecules originating from the water-splitting process at PSII are reduced to water by electrons originating from PSI. This process is termed the water-water cycle (WWC) that is thought to protect the photosynthetic apparatus from excessive light and alleviate photoinhibition.

In the classical WWC, the Mehler-ascorbate peroxidase (MAP) pathway, ascorbate peroxidases (APXs) have been considered as key enzymes in the reductive detoxification of $H_2O_2$ in chloroplasts (Kangasjärvi et al., 2008). APXs reduce $H_2O_2$ to water and oxidize ascorbate to monodehydroascorbate radicals. NADPH functions as an electron donor to regenerate ascorbate by monodehydroascorbate radical reductase. There are two functional APX homologs in plastids: a 33-kD stromal ascorbate peroxidase (sAPX) and a 38-kD thylakoid ascorbate peroxidase (tAPX). The latter tAPX is thought to reside close to the site of $H_2O_2$ generation at PSI. Surprisingly, knockout-tAPX mutants as well as double mutants lacking both the tAPX and the sAPX exhibited no visible symptoms of stress after long-term (1–14 d) HL (1.000 $\mu$mol photons $m^{-2}$ $s^{-1}$) exposure (Giacomelli et al., 2007; Kangasjärvi et al., 2008; Maruta et al., 2010). Moreover, the photosynthetic efficiency of PSII (as judged by the maximum photochemical efficiency of PSII in the dark-adapted state [$F_v/F_m$]), $H_2O_2$ production, antioxidant levels (ascorbate, glutathione, and tocopherols), protein oxidation, and anthocyanin accumulation were similar between light-stressed mutant and wild-type plants. Hence, other $H_2O_2$ detoxification mechanisms can efficiently compensate for the lack of the sAPX and tAPX detoxification system.

In addition to APX, glutathione peroxidases and PRXs may reduce $H_2O_2$ to water. It has been postulated that, in the chloroplast, two highly homologous thylakoid-associated 2-Cys peroxiredoxins (2CPs), 2CPA and 2CPB, can create an alternative ascorbate-independent WWC (Dietz et al., 2006). In support of this concept, HL stress-acclimated *tapx sapx* double-mutant plants showed increased levels of 2-Cys PRX compared with wild-type plants (Kangasjärvi et al., 2008). Because the two plastidial 2CPA and 2CPB dynamically interact with the stromal side of thylakoid membranes and are capable of reducing peroxides, 2-Cys PRX enzymes may be involved in both $H_2O_2$ detoxification and reduction of lipid peroxides in thylakoids (König et al., 2002).

The reaction mechanism of 2-Cys PRX is highly conserved and involves a Cys residue, which becomes transiently oxidized to sulphenic acid (termed the peroxidatic Cys residue), thereby reducing $H_2O_2$ to water. The sulphenic acid is subsequently attacked by a second Cys residue, termed resolving Cys residue, yielding an intermolecular disulfide bridge and water (Dietz, 2011).

At high peroxide concentrations, the peroxidase function of 2-Cys PRX becomes inactivated through overoxidation, and excess $H_2O_2$ may function as a redox signal (Puerto-Galán et al., 2013). It has been postulated that 2-Cys PRXs function as a floodgate that allows $H_2O_2$ signaling only under oxidative stress conditions (Wood et al., 2003; Dietz, 2011; Puerto-Galán et al., 2013). In addition to its function as peroxidase, 2-Cys PRX may also serve as proximity-based thiol oxidases and chaperones (König et al., 2013).

The genome of Arabidopsis (*Arabidopsis thaliana*) contains two *2CP* genes. To study 2-Cys PRX function, transgenic plants with reduced 2-Cys PRX levels were generated by antisense suppression (Baier et al., 2000) as well as crossing of transfer DNA (T-DNA) insertion mutants (Pulido et al., 2010). The T-DNA insertion double mutant was shown to contain less than 5% of the wild-type content of 2CPA and no 2CPB. Hence, full knockout lines lacking both 2-Cys PRXs have not yet been established. Under standard growth conditions, 2-Cys PRX double mutants (similar to plastid APX-deficient plants) also did not show a photooxidative stress phenotype that might be because of compensation by alternative $H_2O_2$ reduction systems (Pulido et al., 2010). Because of the lack of a clear phenotype of the 2-Cys PRX double-knockdown mutant under ML conditions, the physiological functions of 2CPA and 2CPB remain to be elucidated.

The main aim of this study was to identify the physiological function of 2CPA and 2CPB under HL stress conditions, when the WWC is of particular importance in protecting the photosynthetic apparatus from photooxidative damage. We investigated mutants completely deficient in 2-Cys PRX (*2cpa 2cpb*) or tAPX (*tapx*) and in addition, *2cpa 2cpb tapx* triple knockout plants to study the extent of the functional overlap between these enzymes. Results suggest that 2-Cys PRXs are involved in a 2-Cys PRX-dependent WWC that seems to be more important in protecting the photosynthetic apparatus than the tAPX-dependent WWC, the MAP cycle.

## RESULTS

### HL Exposure of *2cpa 2cpb* Double- and *2cpa 2cpb tapx* Triple-Knockout Mutants Causes Photosynthetic Impairment and Photobleaching

To clarify the specific functional role of 2-Cys PRX compared with tAPX in protecting the photosynthetic tissue from photooxidative damage, we generated a double-knockout mutant *2cpa 2cpb* of Arabidopsis completely lacking the plastidial 2CPA and 2CPB (Supplemental Fig. S1) and compared its HL stress responses with those of a mutant line (*tapx*) that does not express *tAPX* (Maruta et al., 2010). In addition, a triple-knockout mutant line, *2cpa 2cpb tapx*, lacking both 2-Cys PRXs and tAPX was generated to study the effect of the loss of both membrane-associated peroxide detoxification systems.

The *2cpa 2cpb* double and the *2cpa 2cpb tapx* triple mutants were selected on Murashige and Skoog (MS) medium containing 1% (w/v) Suc. Unlike wild-type plants as well as single *2cpa* and *2cpb* mutant lines, cotyledons of the *2cpa 2cpb* double and *2cpa 2cpb tapx* triple mutants bleached, and seedlings remained small during early development under these growth conditions. Only 4 plants of 201 individuals of a segregating *2cpa 2cpb* progeny survived. Germination and growth of the double and triple mutants on MS medium without sugar or supplemented with 3% (w/v) sorbitol were similar to the

wild type and the *tapx* mutant line (Supplemental Fig. S2). It is, therefore, likely that growth on Suc rather than osmotic stress is responsible for this phenotype.

Mutant plants completely deficient in 2-Cys PRX (*2cpa 2cpb*) or both 2-Cys PRX and tAPX (*2cpa 2cpb tapx*) grown on soil showed growth retardation, whereas the *tapx* mutant grew like the wild type (Fig. 1A). In *2cpa 2cpb* plants, growth retardation was more pronounced under long- compared with short-day conditions (Supplemental Fig. S3). Under standard growth conditions, *2cpa 2cpb* mutant plants displayed a pale-green leaf phenotype with reduced chlorophyll content, the latter of which was also previously noted in the 2-Cys PRX double-knockdown mutant (Pulido et al., 2010). Compared with the wild type, the ratio of chlorophyll *a* to chlorophyll *b* was not significantly different in the 2-Cys PRX double mutant (Supplemental Fig. S3).

Under HL (900 $\mu$mol $m^{-2}$ $s^{-1}$) conditions, leaves of wild-type and *tapx* plants showed no photooxidative damage, whereas extensive photobleached lesions at the edges of older leaves were observed already after 1 d of HL treatment in the *2cpa 2cpb tapx* triple mutant and *2cpa 2cpb* double-mutant leaves after 2 d of HL exposure (Fig. 1A).

To assess HL-induced photoinhibition of PSII, the maximal quantum yield after dark acclimation ($F_v/F_m$) was determined using chlorophyll fluorescence measurements in the dark with a pulse-amplitude modulation (PAM) fluorometer by implementing the saturation pulse method (Schreiber, 2004). In plants grown under ML (160 $\mu$mol $m^{-2}$ $s^{-1}$), the $F_v/F_m$ ratio (0.77) did not differ between the wild type and all mutant lines. After 1 d of exposure to HL (900 $\mu$mol $m^{-2}$ $s^{-1}$), the $F_v/F_m$ ratio of the wild type and the *tapx* mutant declined to 0.60, whereas the $F_v/F_m$ ratio of the *2cpa 2cpb* and the *2cpa 2cpb tapx* mutants decreased to 0.44 and 0.40, respectively. The maximal quantum yield of PSII did not further decrease in the wild type and the *tapx* mutant after 2 d of HL. In contrast, the $F_v/F_m$ ratio of the *2cpa 2cpb* and the *2cpa 2cpb tapx* mutants further decreased to 0.36 and 0.06, respectively, after 2 d of HL treatment (Fig. 1B), indicating that the PSII of the *2cpa 2cpb* double and the *2cpa 2cpb tapx* triple mutants is more sensitive to HL stress than that of the wild type.

Ultimately, under steady-state conditions of illumination, most electrons are delivered to the carbon-fixating Calvin cycle or photorespiration through the linear electron flow from PSII through PSI and Fd. After continuous ML or 1 d of HL illumination, carbon dioxide fixation rates of the wild type and the *2cpa 2cpb* double mutant were similar, suggesting that the activity of the Calvin cycle is not compromised in the *2cpa 2cpb* double mutant (Fig. 1C). However, after 2 d of HL treatment, carbon dioxide fixation was reduced in the double mutant relative to the wild type, suggesting a late impairment of the Calvin cycle when leaves become photobleached.

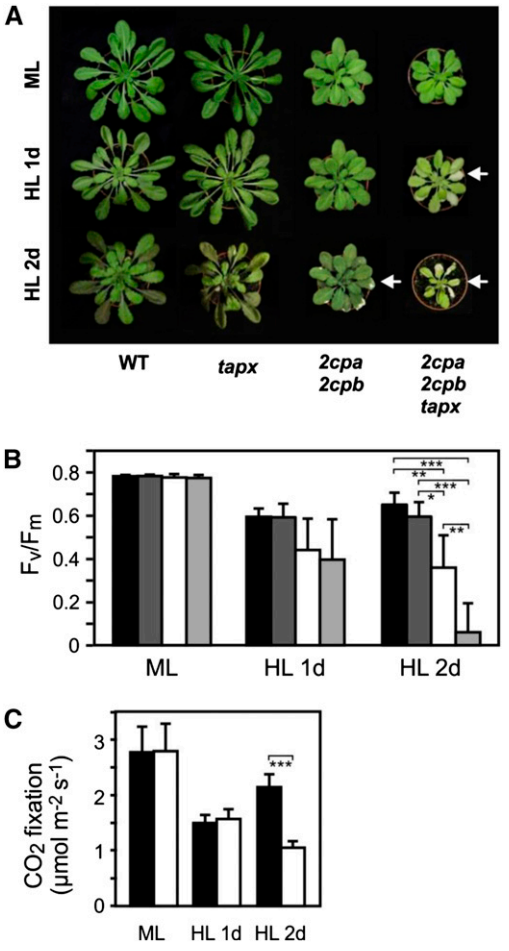


**Figure 1.** HL sensitivity and photosynthetic impairment of *2cpa 2cpb* and *2cpa 2cpb tapx* mutant plants. Wild-type and mutant plants were grown under ML (160 $\mu$mol $m^{-2}$ $s^{-1}$; 8 h $d^{-1}$) and treated with HL (900 $\mu$mol $m^{-2}$ $s^{-1}$; 8 h $d^{-1}$). A, *2cpa 2cpb* and *2cpa 2cpb tapx* plants displayed a smaller habitus with pale green leaves compared with wild-type and *tapx* plants. Leaves of wild-type and *tapx* plants were tolerant to HL, whereas *2cpa 2cpb* and *2cpa 2cpb tapx* plants became partially photobleached after 1 d (*2cpa 2cpb tapx*) or 2 d (*2cpa 2cpb*) of HL treatment. B, Optimal quantum yield ($F_v/F_m$) of wild-type (black bars), *tapx* (dark-gray bars), *2cpa 2cpb* (white bars), and *2cpa 2cpb tapx* (light-gray bars) plants grown under ML or HL conditions. Shown are means ± SD ($n$ = 6). C, Carbon dioxide fixation rate in wild-type (black bars) and *2cpa 2cpb* mutant (white bars) plants grown under ML or HL conditions. The rate of carbon dioxide uptake was determined by gas exchange measurements using an infrared gas analyzer. Shown are means ± SD ($n$ = 3). Significant differences between mean values are indicated by asterisks using Student's $t$ test. WT, Wild type; *, $P < 0.05$; **, $P < 0.01$; ***, $P < 0.001$.

### Superoxide Anion Accumulation, Oxidative Stress, and Protein Oxidation in the *2cpa 2cpb* and *2cpa 2cpb tapx* Mutants

Alternative electron flows are of particular importance under HL conditions. A potential alternative electron flow could be the Mehler reaction (i.e. the transfer of electrons to molecular oxygen), thereby producing superoxide at PSI. By performing nitroblue tetrazolium (NBT) staining, indicative of $O_2\cdot^-$ production, the *2cpa 2cpb* double and *2cpa 2cpb tapx* triple mutants were found to produce more $O_2\cdot^-$ than wild-type and *tapx* mutant plants already under ML (Fig. 2). Under HL illumination, increased $O_2\cdot^-$ formation could be detected in the wild type and *tapx* mutant plants. Highest $O_2\cdot^-$ generation

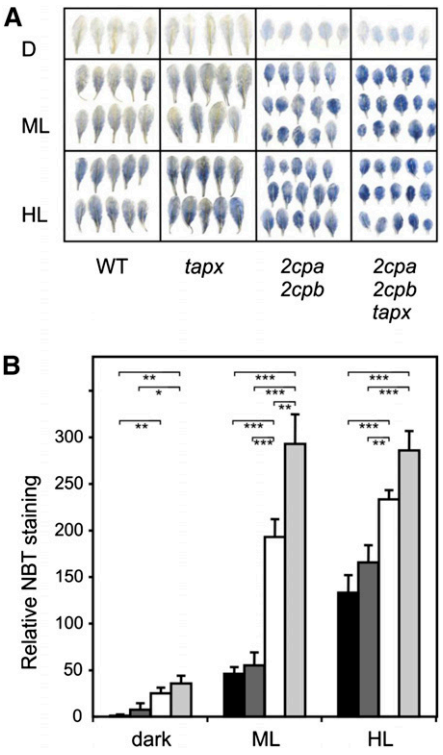


**Figure 2.** Light-induced superoxide anion radical accumulation in wild-type and mutant plants. $O_2\cdot^-$ accumulation in dark-adapted leaves of wild-type (black bars), *tapx* (dark-gray bars), *2cpa 2cpb* (white bars), and *2cpa 2cpb tapx* (light-gray bars) mutant plants was visualized by NBT staining in the dark or after 1 h of ML (160 $\mu$mol $m^{-2}$ $s^{-1}$) or HL (900 $\mu$mol $m^{-2}$ $s^{-1}$) treatment. A, Representative images of stained leaves after chlorophyll extraction. B, Relative NBT staining (integration of blue color density per leaf area) was determined using the ImageJ image processing software. Shown are means ± SE ($n$ = 10). Significant differences between mean values are indicated by asterisks using Student's $t$ test. D, Dark; WT, wild type; *, $P < 0.05$; **, $P < 0.01$; ***, $P < 0.001$.

could be detected in the *2cpa 2cpb* and *2cpa 2cpb tapx* mutant plants. Compared with ML conditions, however, little or no additional increase of the staining could be measured, possibly because of signal saturation (Fig. 2).

Light-induced overaccumulation of $O_2\cdot^-$ in the *2cpa 2cpb* double and *2cpa 2cpb tapx* triple mutants may contribute to photobleaching of leaf tissues observed after 1 to 2 d of HL exposure (Fig. 1). To further estimate the extent of oxidative stress, we determined leaf autoluminescence as a marker of oxidative stress and lipid peroxidation (Havaux et al., 2006). Autoluminescence of wild-type and mutant plants exposed to ML or HL was detected with a CCD camera. Unlike the wild-type and *tapx* mutant plants, *2cpa 2cpb* double and *2cpa 2cpb tapx* triple mutant plants exhibited strong autoluminescence under HL conditions (Fig. 3A).

Oxidative stress-induced increase in autoluminescence has been correlated with lipid peroxidation, although oxidized proteins can also participate in the signal (Birtic et al., 2011). Therefore, protein carbonylation as an indicator of oxidative protein damage (Suzuki et al., 2010) was determined using a highly sensitive chemiluminescence immunoassay that allows us to detect basal protein carbonylation, even in unstressed wild-type Arabidopsis leaves. To avoid signal saturation in samples from the mutants, chemoluminescent immunoblots were only briefly exposed to the detection film. In agreement with the autoluminescence data, we observed no apparent chemiluminescence signals under ML conditions in all genotypes. Under HL conditions, protein carbonylation was detectable in *2cpa 2cpb* and even more pronounced in *2cpa 2cpb tapx* mutants, whereas there was comparably little protein modification in wild-type and *tapx* plants (Fig. 3B). Collectively, these data suggest that complete loss of 2-Cys PRX activity results in increased formation of $O_2\cdot^-$, oxidative stress, and protein oxidation.

### Wild Type-Like Lipid Peroxidation in the *2cpa 2cpb* Mutant in Response to HL Stress

Induction of autoluminescence under HL conditions in *2cpa 2cpb* and *2cpa 2cpb tapx* mutant plants suggested

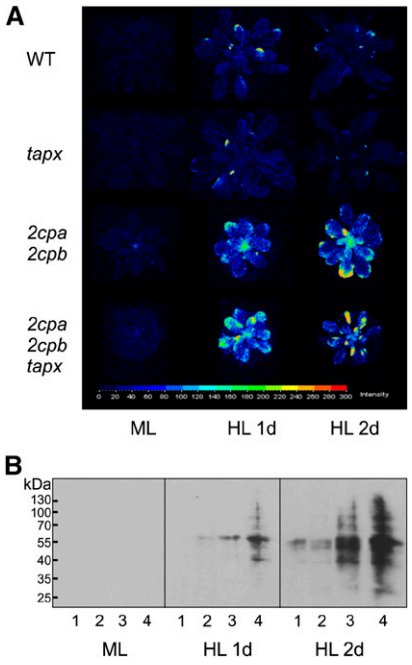


**Figure 3.** Sensitivity of wild-type (WT) and mutant plants to HL stress. A, Autoluminescence of wild-type, *tapx*, *2cpa 2cpb*, and *2cpa 2cpb tapx* mutant plants after 8 h of ML (160 $\mu$mol $m^{-2}$ $s^{-1}$) or 1 or 2 d of HL (900 $\mu$mol $m^{-2}$ $s^{-1}$; 8 h $d^{-1}$) treatment. Images were taken with a CCD camera after 40 min of dark adaptation. Representative pictures from nine measurements were converted to false-color images indicating the relative autoluminescence intensity. B, Effect of light treatment on protein carbonylation in wild-type (1), *tapx* (2), *2cpa 2cpb* (3), and *2cpa 2cpb tapx* (4) plants. Proteins (15 $\mu$g of total protein) were derivatized with 2,4-dinitrophenylhydrazine and subjected to SDS-PAGE. Immunoblotting was performed using an antidinitrophenylhydrazone antibody. Representative blots from three experiments are shown.

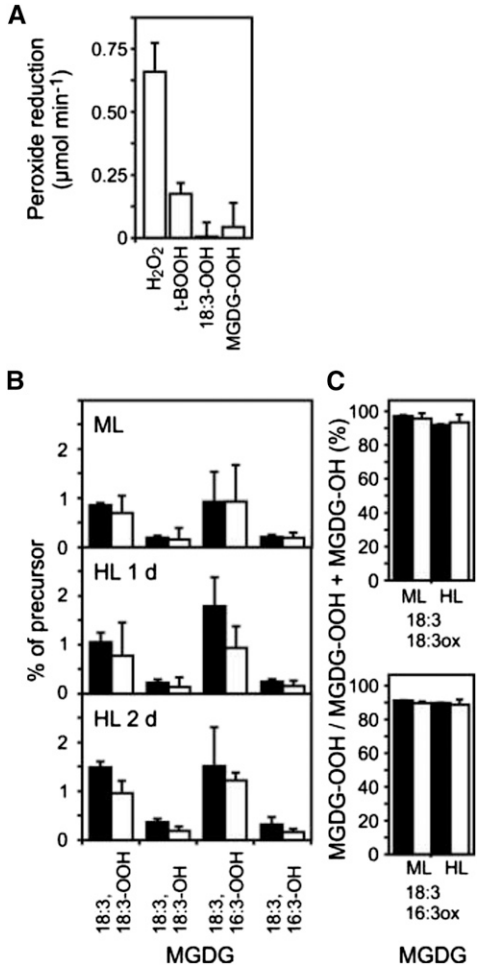


**Figure 4.** Lipid peroxide reduction by 2-Cys PRX. A, The initial rate of peroxide reduction by 2CPA was determined in vitro using 100 $\mu$M DTT as reductant and the following substrates: $H_2O_2$ (25 $\mu$M), *t*-BOOH (25 $\mu$M), 13-hydroperoxy octadecatrienoic acid (HOO-18:3; 25 $\mu$M), and peroxidized MGDGs (HOO-MGDG; 2.5 $\mu$M). Purified recombinant His-tagged 2CPA (5 $\mu$M protein) was used in the assays. B, Wild-type (black bars) and *2cpa 2cpb* (white bars) mutant plant leaves were exposed to ML (160 $\mu$mol $m^{-2}$ $s^{-1}$; 8 h $d^{-1}$) or HL (900 $\mu$mol $m^{-2}$ $s^{-1}$; 8 h $d^{-1}$). The ratios of MGDG peroxides (MGDG-OOH) and hydroxides (MGDG-OH) relative to their nonoxidized MGDG precursors were determined for the indicated MGDG species. C, The ratio of MGDG peroxides relative to total oxidized MGDG is shown for the indicated MGDG species. All values shown are means ± SD ($n$ = 3).

that lipid peroxidation products may accumulate in *2cpa 2cpb* mutant plants in response to HL stress. In vitro, 2-Cys PRXs have previously been shown to reduce not only $H_2O_2$ but also, synthetic alkyl peroxides (König et al., 2002). The predominant plastid lipid peroxides in vivo are monogalactosyldiacylglycerols (MGDGs) with the acyl-chain combination 18:3, 18:3 and 18:3, 16:3, in which one acyl chain is peroxidized (Zoeller et al., 2012).

To assess the capacity of 2-Cys PRXs to reduce naturally occurring MGDG peroxides (MGDG-OOH) to their corresponding hydroxides (MGDG-OH), we incubated recombinant 2CPA with different peroxide substrates and dithiothreitol (DTT) as reductant in vitro. Enzyme assays revealed that the enzyme has a strong preference for $H_2O_2$. The activity of the enzyme toward the artificial peroxide *tert*-butyl hydroperoxide (*t*-BOOH) was less than 30% compared with $H_2O_2$, whereas the activity toward endogenously occurring 13-hydroperoxy octadecatrienoic acid (18:3-OOH) and peroxidized MGDG (MGDG-OOH) was very low (Fig. 4A).

We also determined the levels of the two major MGDG-OOH, (18:3, 18:3-OOH)MGDG and (18:3, 16:3-OOH)MGDG, as well as their reduced metabolites, (18:3, 18:3-OH)MGDG and (18:3, 16:3-OH)MGDG, relative to their nonoxidized precursors, (18:3,18:3)MGDG and (18:3, 16:3)MGDG, in vivo (Fig. 4B). Under ML and HL conditions, we detected comparable levels of oxidized MGDGs in wild-type and *2cpa 2cpb* mutant leaves, indicating wild type-like thylakoid lipid oxidation in the *2cpa 2cpb* mutant (Fig. 4B). Moreover, the percentage of peroxidized MGDG (MGDG-OOH) relative to total oxidized MGDGs (MGDG-OOH + MGDG-OH) was higher than 90% in both genotypes under ML and HL conditions (Fig. 4C). Therefore, MGDG peroxides are, for the most part, not reduced in vivo and do not seem to be major substrates of 2-Cys PRX.

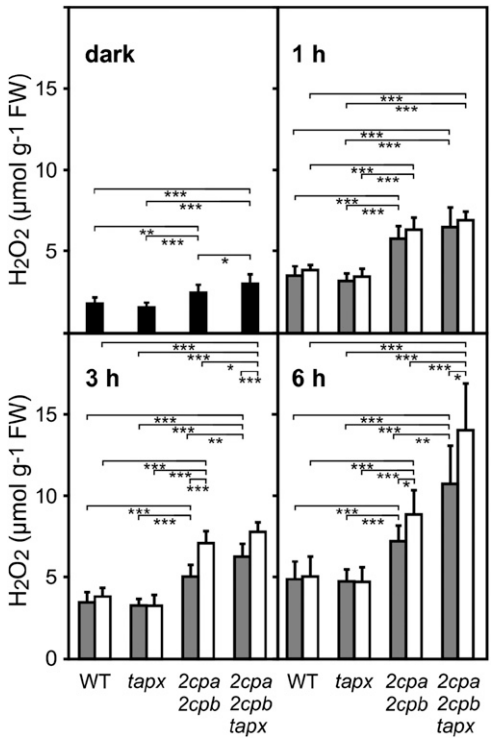


**Figure 5.** Light-induced $H_2O_2$ levels in different genotypes. At the end of the night, leaves of wild-type (WT), *tapx*, *2cpa 2cpb*, and *2cpa 2cpb tapx* plants were kept in the dark (black bars) for 3 h or treated with ML (gray bars; 160 $\mu$mol $m^{-2}$ $s^{-1}$) or HL (white bars; 900 $\mu$mol $m^{-2}$ $s^{-1}$) for the times indicated. Whole-leaf $H_2O_2$ levels were determined using the homovanillic acid fluorescence assay. All values shown are means ± SD ($n$ = 10). Significant differences between mean values are indicated by asterisks using Student's $t$ test. FW, Fresh weight; *, $P < 0.05$; **, $P < 0.01$; ***, $P < 0.001$.

### Light-Induced $H_2O_2$ Overaccumulation in *2cpa 2cpb* and *2cpa 2cpb tapx* Mutant Plants

Compared with wild-type and *tapx* leaves, *2cpa 2cpb* and *2cpa 2cpb tapx* mutant leaves are expected to accumulate more $H_2O_2$ in the absence of the $H_2O_2$-detoxifying enzymes 2-Cys PRX and tAPX. To determine light-induced $H_2O_2$ levels in wild-type, *tapx*, *2cpa 2cpb*, and *2cpa 2cpb tapx* leaves, whole-leaf $H_2O_2$ levels were quantitated with the homovanillic acid fluorescence assay (Creissen et al., 1999). In wild-type and *tapx* leaves, $H_2O_2$ levels were low under dark conditions (1.6–1.8 $\mu$mol $g^{-1}$ fresh weight) and displayed higher $H_2O_2$ levels under ML and HL conditions (4.7–5 $\mu$mol $g^{-1}$ fresh weight after 6 h). Compared with wild-type plants, *2cpa 2cpb* mutant plants displayed slightly elevated $H_2O_2$ levels (2.5 $\mu$mol $g^{-1}$ fresh weight) already in the dark (Fig. 5). Levels of $H_2O_2$ further increased to 7.2 and 8.8 $\mu$mol $g^{-1}$ fresh weight under ML and HL conditions (6 h), respectively. In the *2cpa 2cpb tapx* mutant, levels of $H_2O_2$ were found to be 3.0, 10.7, and 14.0 $\mu$mol $g^{-1}$ fresh weight under dark, ML, and HL conditions (6 h), respectively (Fig. 5). Although the wild type and the *tapx* mutant maintained $H_2O_2$ levels below or at 5 $\mu$mol $g^{-1}$ fresh weight upon HL treatment, *2cpa 2cpb* and *2cpa 2cpb tapx* mutants were unable to confine $H_2O_2$ levels below the 5 $\mu$mol $g^{-1}$ fresh weight wild-type limit already under ML conditions (Fig. 5). $H_2O_2$ levels further increased in both mutants when exposed to HL.

Hence, with respect to HL-induced accumulation of $H_2O_2$ (Fig. 5), lack of tAPX seemed to be fully compensated by 2-Cys PRX. In contrast, lack of 2-Cys PRX could only partially be compensated by tAPX, because mutants lacking both 2-Cys PRX and tAPX displayed higher $H_2O_2$ levels than mutants deficient in 2-Cys PRX under ML and HL conditions.

### 2-Cys PRX and tAPX Restrict Redox-Regulated Gene Expression in Response to HL Stress

It has been proposed that 2-Cys PRX might be involved in ROS-mediated retrograde signaling. We, therefore, compared the response of ROS-inducible genes with HL treatment in wild-type, *tapx*, *2cpa 2cpb*, and *2cpa 2cpb tapx* plants. Among ROS-induced genes, many heat shock genes, including *HEAT SHOCK FACTOR A2* (*HSFA2*) and *HEAT SHOCK PROTEIN101* (*HSP101*), are early stress-responsive genes that are transiently up-regulated (displaying maximal expression 1 after onset of HL) by not only heat stress but also, $H_2O_2$ (Davletova et al., 2005; Maruta et al., 2010). In wild-type, *tapx*, and *2cpa 2cpb* plants, we could not determine a strong induction of *HsfA2* and *Hsp101* under HL conditions, whereas a transient and dramatic up-regulation of these genes was measured in the *2cpa 2cpb tapx* triple-mutant plants (Fig. 6). A strong and significant induction of the redox- and $H_2O_2$-responsive genes *OXIDATIVE SIGNAL-INDUCIBLE1* (*OXI1*), *ZINC FINGER PROTEIN12* (*ZAT12*), and *At1g49150* (unknown protein) as well as the singlet oxygen-responsive genes *OXI1* and *BON ASSOCIATION PROTEIN1* (*BAP1*; Davletova et al., 2005; Queval et al., 2007; Triantaphylidès et al., 2008) by HL was also observed in the *2cpa 2cpb tapx* mutant. In contrast, wild-type, *tapx*, and *2cpa 2cpb* plants did not up-regulate or only slightly up-regulated these redox- and ROS-responsive genes under HL conditions (Fig. 6). These data suggest that lack of either 2-Cys PRXs or tAPX alone is not sufficient to trigger these genes in Arabidopsis in response to HL.

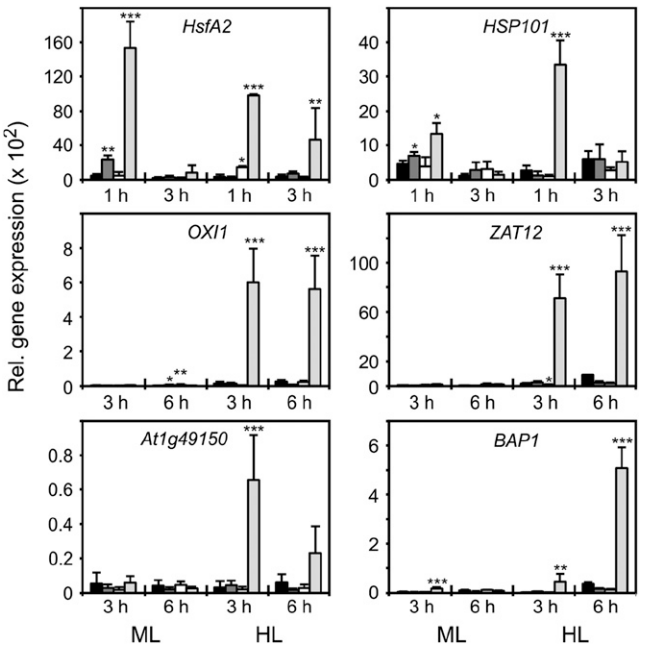


**Figure 6.** HL-induced expression of redox-regulated genes in wild-type and mutant plants. Expression of *HSFA2*, *HSP101*, *OXI1*, *ZAT12*, *At1g49150*, and *BAP1* in wild-type (black bars), *tapx* (dark-gray bars), *2cpa 2cpb* (white bars), and *2cpa 2cpb tapx* (light-gray bars) plants after ML (160 $\mu$mol $m^{-2}$ $s^{-1}$) or HL (900 $\mu$mol $m^{-2}$ $s^{-1}$) treatment for the times indicated. Expression was normalized to the actin gene *ACTIN2/ACTIN8*. All values shown are means ± SD ($n = 3$). Significant differences between mean values of wild-type and mutant plants are indicated by asterisks using Student's *t* test. *, $P < 0.05$; **, $P < 0.01$; ***, $P < 0.001$.

### 2CPA and 2CPB Are Essential for HL-Induced Anthocyanin Accumulation

We observed that wild-type and *tapx* plants accumulated purple pigments, indicative for anthocyanin biosynthesis, after 2 d of HL treatment. In contrast, there was little increase of pigmentation in *2cpa 2cpb* and *2cpa 2cpb tapx* mutant plants (Supplemental Fig. S4A). Anthocyanin quantification revealed that anthocyanin levels increased 8.8-fold in the wild type and only 2.6-fold in *2cpa 2cpb* mutant plants after 3 d of HL exposure (Fig. 7A). To discern differences in the regulation of anthocyanin biosynthesis between wild-type and *2cpa 2cpb* mutant plants, gene expression and metabolic profiles were assessed in

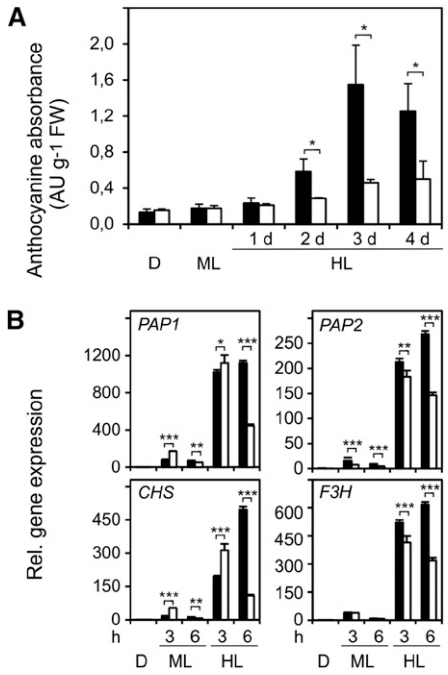


**Figure 7.** Light-induced anthocyanin content and anthocyanin-related gene expression in wild-type and *2cpa 2cpb* plants. A, Anthocyanin accumulation in wild-type (black bars) and *2cpa 2cpb* mutant (white bars) plants after the dark period (16 h), ML (8 h $d^{-1}$; 160 $\mu$mol $m^{-2}$ $s^{-1}$), or HL (8 h $d^{-1}$; 900 $\mu$mol $m^{-2}$ $s^{-1}$). B, Quantitative reverse transcription PCR analysis of regulatory and structural genes contributing to anthocyanin biosynthesis in wild-type (black bars) and *2cpa 2cpb* mutant (white bars) plants after darkness, ML, and HL treatment. Expression of the *PAP1*, *PAP2*, *CHS*, and *FSH* genes was normalized to the *ACTIN2/ACTIN8* genes. Expression in wild-type leaves after dark was arbitrarily set to one, and all other expression values were expressed relative to it. All values shown are means ± SD ($n$ = 3). Significant differences between mean values are indicated by asterisks using Student's $t$ test. D, Dark; FW, fresh weight; *, $P < 0.05$; **, $P < 0.01$; ***, $P < 0.001$.

the dark and after ML or HL treatment. Expression of the HL-induced regulatory genes *PRODUCTION OF ANTHOCYANIN PIGMENT1* (*PAP1*) and *PAP2* and the structural *CHALCONE SYNTHASE* (*CHS*) and *FLAVANONE 3-HYDROXYLASE* (*F3H*) genes increased continuously when wild-type plants were exposed for 6 h to HL (Fig. 7B). In contrast, expression of all four genes only transiently increased in the *2cpa 2cpb* double mutant, reaching maximal mRNA abundance after 3 h of HL exposure. In addition, levels of aromatic amino acids, including Phe, a precursor of anthocyanins, increased in the wild type but not *2cpa 2cpb* mutant plants in response to HL (Supplemental Fig. S4B). These data suggest that a sustained activation of anthocyanin biosynthesis genes and accumulation of amino acid precursors do not occur in the *2cpa 2cpb* double mutant.

HL-induced anthocyanin accumulation can be repressed by elevated intracellular $H_2O_2$ levels (Vandenabeele et al., 2004; Vanderauwera et al., 2005). Because $H_2O_2$ levels are higher in the *2cpa 2cpb* and *2cpa 2cpb tapx* mutant plants compared with wild-type and *tapx* mutant plants, $H_2O_2$-mediated down-regulation of the entire anthocyanin biosynthesis pathway may suppress anthocyanin accumulation in 2-Cys PRX-deficient plants. Potentially, other mechanisms may contribute to anthocyanin suppression in *2cpa 2cpb* mutant plants. It has been shown that ascorbate deficiency or perturbations of the cellular redox status (Giacomelli et al., 2006; Page et al., 2012) are associated with reduced anthocyanin accumulation. To this end, analysis of the levels of soluble antioxidants revealed that absolute levels of reduced glutathione and ascorbate were slightly lower in *2cpa 2cpb* mutant compared with wild-type plants under ML conditions but did not significantly differ between the genotypes during HL treatment. Moreover, the ratio of the oxidized and reduced forms of both metabolites was similar for wild-type and *2cpa 2cpb* double-mutant plants (Supplemental Fig. S5). Jasmonates have also been implicated in mediating stress-induced anthocyanin accumulation (Shan et al., 2009). Therefore, the effect of HL stress on the levels of these oxylipins was determined in the wild type and the *2cpa 2cpb* mutant plants. However, HL stress induced a similar accumulation of jasmonic acid and jasmonic acid-Ile in both the wild type and 2-Cys PRX-deficient plants (Supplemental Fig. S5).

## DISCUSSION

### 2-Cys PRX Enzymes Are Essential and More Important Than tAPX for the Function of the WWC and Photoprotection under HL Conditions

Several functions have been proposed for 2-Cys PRX. Because 2-Cys PRXs have been shown to reduce a broad range of peroxides, including $H_2O_2$, and synthetic alkyl hydroperoxides, such as butyl or cumene hydroperoxides, they may be involved in detoxification of plastid $H_2O_2$ and membrane lipid peroxides (König et al., 2002; Rouhier and Jacquot, 2002). It has also been suggested that 2-Cys PRXs function in an alternative ascorbate-independent WWC (König et al., 2002; Dietz et al., 2006) in addition to the classical WWC, the MAP cycle (Fig. 8), because 2-Cys PRXs can also use electrons delivered from the photosynthetic electron transport chain to reduce $H_2O_2$.

The classical ascorbate-dependent WWC involves plastid sAPX and tAPX, from which the thylakoid-bound tAPX at the site of $H_2O_2$ generation seems to be most important (Maruta et al., 2010; Miyake, 2010). However, recent studies using Arabidopsis *sapx tapx* double mutants suggested that plastid APXs are not key enzymes in photoprotection, because the double-knockout mutants exhibited no visible symptoms of stress after long-term (1–14 d) HL (up to 2.000 $\mu$mol photons $m^{-2}$ $s^{-1}$) exposure (Giacomelli et al., 2007; Kangasjärvi et al., 2008; Maruta et al., 2010). At least under standard growth conditions, double-mutant 2-Cys PRX-deficient plants with less than 5% 2-Cys PRX content also did not display visible photooxidative damages (Pulido et al., 2010).

To clarify the role of tAPX and 2-Cys PRX in the WWC, we analyzed wild-type plants and mutants deficient in tAPX (*tapx*), 2-Cys PRXs (*2cpa 2cpb*), or tAPX and 2-Cys PRXs (*2cpa 2cpb tapx*) under not only normal but also HL

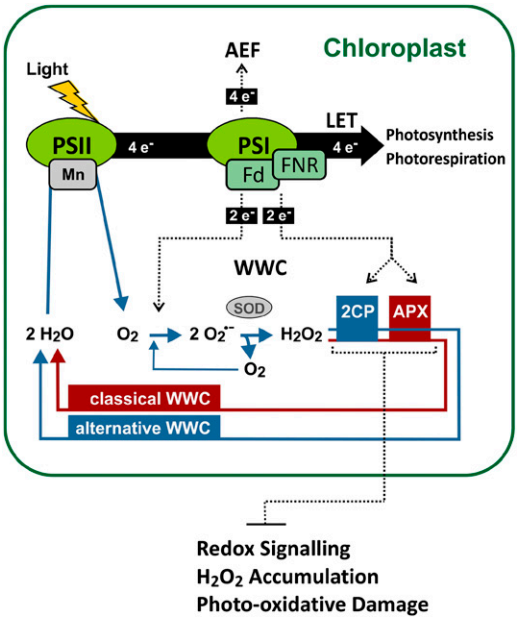


**Figure 8.** Model of the photoprotective function of 2-Cys PRX and tAPX. The WWC and other alternative electron flows (AEFs) are proposed to prevent overreduction of the linear electron transport chain (LET) and protect the photosystems from oxidative damage. Under HL conditions, 2CPs are essential for maintaining a WWC and more important than plastid APX involved in the classical WWC for protection of the photosystems. 2-Cys PRX and tAPX synergistically inhibit activation of redox-responsive genes and prevent overaccumulation of $H_2O_2$ as well as photooxidative damage under HL conditions. FNR, Fd NADP oxidoreductase; SOD, superoxide dismutase.

conditions. Under these conditions, the WWC is important for the dissipation of excess photon energy and the maintenance of the electron flow for building up a pH gradient that facilitates other mechanisms of nonphotochemical energy quenching. It also serves as an electron sink, preventing electron carriers from being overreduced, which would facilitate $O_2\cdot^-$ formation and damage development (Miyake, 2010).

In agreement with the literature (Giacomelli et al., 2007; Kangasjärvi et al., 2008; Maruta et al., 2010), *tapx* mutant plants displayed no or little apparent phenotypic differences to wild-type plants under ML and HL conditions. As previously noted in antisense-suppressed 2-Cys PRX lines (Baier et al., 2000), we observed growth retardation of *2cpa 2cpb* and *2cpa 2cpb tapx* mutant plants under standard growth conditions (Fig. 1A). Under these conditions, mutant plants almost deficient in 2-Cys PRX were shown to accumulate slightly more $H_2O_2$ and 4.7-fold more carbonylated proteins than wild-type plants (Pulido et al., 2010). However, increased levels of $H_2O_2$ and carbonylated proteins in the mutant were not associated with PSII photoinhibition (as indicated by the $F_v/F_m$ value) and photobleaching under ML (Pulido et al., 2010). We obtained similar results when studying mutants completely deficient in 2-Cys PRX. However, we did not observe an accumulation of carbonylated proteins under our standard growth conditions.

When compared under HL conditions, *2cpa 2cpb* mutant plants showed an impairment in PSII photochemical efficiency (Fig. 1B) and an increased formation of superoxide anion radicals (Fig. 2) and $H_2O_2$ (Fig. 5). As a consequence, *2cpa 2cpb* mutants suffered from massive oxidative stress, which was indicated by elevated autoluminescence and protein carbonylation (Fig. 3), and are, ultimately, photobleached under HL conditions (Fig. 1). As described in the literature (Giacomelli et al., 2007; Kangasjärvi et al., 2008), *tapx* mutant plants behaved like the wild type and did not show any of these symptoms under HL conditions. These experiments indicate that 2-Cys PRXs are essential and more important than tAPX in preventing excessive $O_2\cdot^-$ and $H_2O_2$ formation (Figs. 2 and 5) as well as photooxidative damage (Figs. 1 and 3) under HL conditions. Notably, transcription of several *APX* genes, including *tAPX*, as well as the enzyme activities of Cu/ZnSOD and APX have been shown to be down-regulated in 2-Cys PRX-deficient mutants already under normal light conditions (Pulido et al., 2010). Notably, knockdown Arabidopsis plants with suppressed expression of Cu/ZnSOD display growth retardation and reduced chlorophyll content and photosynthetic activity (Rizhsky et al., 2003). Hence, the constitutive reduced capacity to detoxify $O_2\cdot^-$ and $H_2O_2$ by these enzymes in the mutants may contribute to ROS toxicity and photosensitivity.

In contrast to tAPX, 2-Cys PRXs have been proposed to be involved in the reduction of reactive lipid peroxides, thereby providing an additional layer of antioxidative defense and photosystem protection. However, we did not observe massive increases of lipid peroxides under the applied HL conditions in both wild-type and *2cpa 2cpb* mutant plants (Fig. 4B). Moreover, the ratio of major thylakoid lipid peroxides to their reduced counterparts was not found to be affected in the *2cpa 2cpb* mutant (Fig. 4C), suggesting that $H_2O_2$ rather than lipid peroxide reduction is the major biochemical function of 2-Cys Prx enzymes in vivo.

Other than detoxification of $H_2O_2$, another function of the WWC peroxidases is to serve as electron transmitters that constitute an electron flow in addition to the electron flow provided through the Mehler reaction (Fig. 8). When the linear electron transfer chain becomes overreduced, such as under HL conditions, the electron pressure can partially be relieved through transfer of two electrons from PSI to $O_2$ (e.g. the Mehler reaction), leading to the formation of $O_2\cdot^-$. In addition, the electron pressure at PSI can also be decreased by transfer of two electrons to $H_2O_2$ by using 2-Cys PRX and tAPX as electron transmitters (Fig. 8). We hypothesize that deficiency in 2-Cys PRX increases the electron pressure at PSI, leading to an accelerated Mehler reaction and excessive superoxide accumulation (Fig. 2). As a consequence, more $H_2O_2$ is produced through Cu/ZnSOD-catalyzed or nonenzymatic dismutation of $O_2\cdot^-$ and accumulates, because tAPX and other $H_2O_2$-detoxifying enzymes cannot fully compensate the deficiency in 2-Cys PRX. In the *2cpa 2cpb* mutant, we determined an increase of $H_2O_2$ levels from 2.5 $\mu$mol $g^{-1}$ fresh weight (in the dark) to

8.8 $\mu$mol $g^{-1}$ fresh weight after 6 h under HL conditions (Fig. 5). Because chloroplast enzymes are extremely sensitive to $H_2O_2$, plastid $H_2O_2$ levels are low and have been estimated to be around 0.8 $\mu$M in nonstressed leaves (Asada, 1999). The high levels of $H_2O_2$ that we and others (Pulido et al., 2010) determined already under normal light conditions in whole-leaf extracts (in the millimolar range) are much too high to represent chloroplast $H_2O_2$ levels. Hence, basal- and HL-induced $H_2O_2$ accumulates to a major part outside chloroplasts and may originate only to a minor part—because of the reduced $H_2O_2$ detoxification capacity in the mutants—from chloroplasts. In photosynthetic cells, photorespiratory production of $H_2O_2$ in peroxisomes has been shown to be the major source of $H_2O_2$ (Foyer et al., 2009) and increase under photooxidative stress conditions (Kangasjärvi et al., 2012). The site and mechanism of excessive $H_2O_2$ generation in 2-Cys PRX-deficient mutants are not known but seem to be triggered by disturbance of redox homoeostasis or ROS accumulation in chloroplasts. In addition, constitutive down-regulation of sAPX and tAPX as well as at least five nonplastidic APXs, including cytosolic APX1, APX3, APX4, APX5, and APX6 (Pulido et al., 2010), may limit the capacity to reduce HL-induced $H_2O_2$ in several compartments.

Notably, photorespiratory overproduction of $H_2O_2$ in mutants deficient in peroxisomal catalases has been shown to inhibit light-induced accumulation of anthocyanins (Vandenabeele et al., 2004; Vanderauwera et al., 2005). In 2-Cys PRX-deficient plants, we observed an inhibition of HL-induced anthocyanin accumulation, which is compatible with the hypothesis that $H_2O_2$ overproduction in 2-Cys PRX-deficient mutants could be responsible for the down-regulation of anthocyanin biosynthesis.

### 2-Cys PRX and tAPX Synergistically Restrict Photooxidative Stress Signaling under HL Conditions

A peculiar characteristic of 2-Cys PRX and tAPX is that the enzymes are sensitive to overoxidation and inactivation by $H_2O_2$ (Kitajima, 2008). An $H_2O_2$ floodgate hypothesis has been proposed, according to which $H_2O_2$ acts as a signal in eukaryotic organisms when excessively formed $H_2O_2$ can no longer be detoxified by sensitive 2-Cys PRX because of overoxidation of the peroxidative Cys at the active site of 2-Cys PRX (Wood et al., 2003; Puerto-Galán et al., 2013). Therefore, we tested the floodgate hypothesis in the 2-Cys PRX-deficient mutant. Although we observed higher $H_2O_2$ levels and photooxidative damage in 2-Cys PRX-deficient mutants, we did not observe an overinduction of typical $H_2O_2$-responsive marker genes (Fig. 6) in the *2cpa 2cpb* mutant compared with wild-type plants under HL conditions. Hence, the postulated floodgate preventing $H_2O_2$ signaling does not collapse in the absence of 2-Cys PRX in the mutants.

With respect to tAPX, this enzyme becomes rapidly inactivated by $H_2O_2$ when ascorbate levels fall below a threshold level (Shigeoka et al., 2002). However, we did not measure a significant difference in ascorbate levels between the *2cpa 2cpb* mutant and the wild type (Supplemental Fig. S5). To investigate the functional redundancy of 2-Cys PRX and tAPX, we analyzed *2cpa 2cpb tapx* triple-mutant plants. The triple mutant was more photosensitive than the *2cpa 2cpb* double mutant (Fig. 1), and all indicators of photooxidative damage, including impairment in photosynthetic efficiency, photobleaching, $O_2^{\cdot -}$, and $H_2O_2$ accumulation, were found to be exacerbated (Figs. 1, 2, 3, and 5). Hence, tAPX is at least partially functional in the *2cpa 2cpb* double mutant and attenuates the effects of 2-Cys PRX deficiency. The compensatory function of tAPX may, in particular, be important for maintaining the WWC when 2-Cys Prx become overoxidized and inactivated.

When tAPX become inactivated in addition to 2-Cys PRX, plants may resemble *2cpa 2cpb tapx* triple mutants that display strong up-regulation of photooxidative stress- and $H_2O_2$-responsive marker genes in response to HL. According to the $H_2O_2$ floodgate hypothesis, 2-Cys PRX and tAPX seem to restrict activation of $H_2O_2$-responsive genes, potentially through preventing overaccumulation of $H_2O_2$ in response to HL (Fig. 7). However, despite pronounced differences in the activation of $H_2O_2$-responsive genes, global $H_2O_2$ levels were not found to be that much different between *2cpa 2cpb* and *2cpa 2cpb tapx* mutant plants after 1 and 3 h under HL conditions. Unfortunately, plastid levels of $H_2O_2$ could not be measured directly and may differ more strongly between the mutants than global $H_2O_2$ levels suggest. Therefore, a potential plastid $H_2O_2$ signal may be hidden by the bulk of $H_2O_2$ produced in extrachloroplastic compartments (Fig. 8). Alternatively, the altered plastid redox state or overreduction of photosynthetic electron transport components may generate an $H_2O_2$-independent retrograde plastid to nucleus signal in *2cpa 2cpb tapx* mutant plants that are severely compromised in the WWC alternative electron flow. Recently, it has been shown that overreduction of the plastoquinone pool by the photosynthetic electron transport inhibitor 2,5-dibromo-3-methyl-6-isopropyl-*p*-benzoquinone dramatically induces photooxidative stress- and $H_2O_2$-responsive genes, including *HSFA2*, *HSP101*, *OXI1*, and *ZAT12*, without increasing levels of $H_2O_2$ (Jung et al., 2013).

## CONCLUSION

2-Cys PRXs seem to be essential for optimal function of an alternative electron flow, the WWC, that is important for photoprotection under HL conditions. tAPX seems to be dispensable as long as the 2-Cys PRX system is functional. Because 2-Cys PRXs are sensitive to $H_2O_2$-mediated overoxidation, they may become inactivated under severe photooxidative stress conditions. In this situation, tAPX may partially compensate for the loss of 2-Cys PRX in the WWC. Under severe oxidative stress conditions associated with low ascorbate levels, tAPX may also become inactivated by $H_2O_2$. Loss of both WWC peroxidase systems, the ascorbate-independent 2-Cys PRX and the ascorbate-dependent tAPX, leads to

a condition in which HL strongly activates $H_2O_2$- and photooxidative stress-responsive genes.

## MATERIALS AND METHODS

### Plant Material and Growth Conditions

The Arabidopsis (*Arabidopsis thaliana*) wild type (ecotype Columbia-0) and T-DNA insertion mutants were grown in soil in culture chambers under short-day conditions and ML intensity (160 $\mu$mol $m^{-2}$ $s^{-1}$, 9-h-light/15-h-dark cycle) at 22°C and 20°C during light and dark periods, respectively. Arabidopsis T-DNA insertion lines GK-295C05 (*2-Cys PRXA* gene At3g11630; referred to as *2cpa-2* mutant), SALK_017213C (*2-Cys PRX B* gene At5g06290; referred to as *2cpb-1* mutant), and WiscDsLox457-460A17 (*tAPX* gene At1g77490; referred to as *tapx* mutant) were obtained from the Nottingham Arabidopsis Stock Centre. Homozygous *2cpa-2* and *2cpb-1* mutant plants were crossed to generate the *2cpa 2cpb* double mutant (Supplemental Fig. S1).

The homozygous *2cpa 2cpb* double mutant was crossed with the homozygous *tapx* mutant, resulting in generation of the *2cpa 2cpb tapx* triple mutant. Progeny obtained from these crosses were genotyped for homozygosity in T-DNA insertions using PCR analysis of genomic DNA and primer pairs listed in Supplemental Table S1. Primers, recommended by T-DNA Express: Arabidopsis Gene Mapping Tool, were used for genotyping combined with LBb1.3, 8409, and p745 for SALK, GK, and WiscDsLox lines, respectively. Genomic DNA was extracted using a modified cetyltrimethylammonium bromide-based method (Clarke, 2009). A Nanodrop ND-1000 UV-Vis Spectrophotometer was used for DNA quantification.

Homozygous *2cpa 2cpb* double-mutant and *2cpa 2cpb tapx* triple-mutant plants were selected on MS medium containing 1% (w/v) Suc, and MS medium with 3% (w/v) sorbitol or without Suc served as controls. Seedlings were grown under sterile and short-day conditions (160 $\mu$mol $m^{-2}$ $s^{-1}$; 9-h-light at 22°C/15-h-dark at 20°C cycle).

Plants (6 weeks old) were grown under ML (160 $\mu$mol $m^{-2}$ $s^{-1}$) or HL (900 $\mu$mol $m^{-2}$ $s^{-1}$) stress. Under HL, leaf surface temperature increased to between 28°C and 32°C.

### Heterologous Expression and Purification of Recombinant 2CPA

*Escherichia coli* BL21(DE3) cells expressing His-tagged 2CPA (Horling et al., 2003) were provided by Karl J. Dietz (University of Bielefeld, Germany). $His_6$-tagged 2CPA protein was expressed in *E. coli*, isolated, and purified through immobilized metal ion affinity chromatography as described (Horling et al., 2003).

### Measurement of Chlorophyll Fluorescence

PAM fluorometry was used to measure chlorophyll fluorescence in plants grown under ML or HL. Chlorophyll fluorescence was measured with a Maxi Imaging PAM Chlorophyll Fluorometer (Walz GmbH) using the saturation pulse method as described (Schreiber, 2004; Bonfig et al., 2006). The optimal quantum yield of PSII ($F_v/F_m$) was determined using the software ImagingWin version 2.41a (Walz GmbH) as described (van Kooten and Snel, 1990).

### Carbon Dioxide Uptake Measurements

The uptake of net carbon dioxide by plants was recorded in an open gas exchange system consisting of two parallel water-cooled whole-plant cuvettes using an infrared gas analyzer (HCM-1000; Heinz Walz GmbH). Illumination was provided by three light-emitting diodes, providing light at 655 nm at a photon fluence rate of 100 $\mu$mol $m^{-2}$ $s^{-1}$, 455 nm, and 395 nm at 8 $\mu$mol $m^{-2}$ $s^{-1}$ (Bauer et al., 2013). To avoid introduction of gas exchange caused by soil microorganisms, the potting soil was covered with a black plastic disc and water-tight foil. The gas flow rate through each cuvette was adjusted and controlled by mass flow meters (Red-y Smart Series; www.voegtlin.com). Conditioned air with defined carbon dioxide concentration (380 $\mu$L $L^{-1}$) and gas flow rate (1 L $min^{-1}$) was pumped into the two cuvettes over the leaf rosettes at 24°C and 42% relative humidity. Light conditions were used as described (Bauer et al., 2013). Carbon dioxide uptake was measured in dark-adapted plants after switching on the light. To determine the carbon dioxide uptake, carbon dioxide levels determined in the light were subtracted from the initial ambient carbon dioxide value (380 $\mu$L $L^{-1}$) and related to the leaf rosette surface area calculated using ImageJ software (http://imagej.nih.gov/ij).

### In Situ Superoxide Analysis by NBT Staining

For visualization of superoxide accumulation in leaves, the NBT staining method (Jabs et al., 1996) was used with modifications. Before light treatment, dark-adapted leaves were detached and vacuum infiltrated with freshly prepared 0.1% (w/v) NBT (Sigma Aldrich) in water. To prevent dehydration, leaves were watered through their petioles and kept in darkness for 2 h to allow absorption of the infiltrated NBT solution. Thereafter, NBT-infiltrated leaves were kept in darkness or treated with ML or HL for 1 h. For evaluation of NBT staining, leaves were boiled in a glycerol:lactatophenole:ethanol (1:1:4, v/v/v) solution to remove chlorophyll for 6 min, washed with water, and photographed on white background. Image processing was performed with Corel Draw X5 (for blue color extraction) and ImageJ (National Institute of Mental Health) for integration of the blue pixel density per leaf area (Nguyen, 2013).

### Autoluminescence Measurements

Autoluminescence of plants was detected with a CCD camera (Hamamatsu C4742-98; Hamamatsu Photonics). Plants were first exposed to ML (160 $\mu$mol $m^{-2}$ $s^{-1}$) or HL (900 $\mu$mol $m^{-2}$ $s^{-1}$) for 1 or 2 d and then dark adapted for 40 min for chlorophyll luminescence to decay. The Hokawo 2.1 Imaging Software (Hamamatsu Photonics) was used for image acquisition; the exposure time was 20 min. Images were converted into pseudo colors with an intensity range from 0 to 300.

### Detection of Carbonylated Proteins

Proteins were extracted as described (Lehtimäki et al., 2011) with modifications. Leaves frozen in liquid nitrogen were covered with argon to prevent oxidation, homogenized in liquid nitrogen, and extracted with ice-cold extraction buffer (1:1, w/v) containing 10 mM HEPES-KOH (pH 7.6), 5 mM Suc, and 5 mM $MgCl_2$ using a bead mill for homogenization (21 Hz for 1 min). The homogenate was filtered through miracloth (mesh size, 210 $\mu$m) to remove cell debris. Protein concentration was determined using Bradford reagent and bovine serum albumin as standard (Spector, 1978).

Protein samples were separated by SDS-PAGE (12.5% [w/v] acrylamide). After electrophoresis, the proteins were transferred to a polyvinylidene fluoride membrane (Millipore). Carbonylated proteins were detected using the OxyBlot Protein Oxidation Detection Kit (S7150; Millipore) based on derivatization of carbonyl groups in protein side chains to 2,4-dinitrophenylhydrazone by reaction with 2,4-dinitrophenylhydrazine. Primary antibody specific for the 2,4-dinitrophenylmoiety was used for detection.

### $H_2O_2$ Quantification

$H_2O_2$ was determined by the homovanillic acid oxidation assay (Creissen et al., 1999) with modifications. Leaves were detached, watered through their petioles to prevent dehydration, and kept in the dark or treated with ML or HL for 1, 3, or 6 h. Thereafter, preweighed leaves were shock frozen in liquid nitrogen and ground in a bead mill. The frozen tissue powder (50 mg) was extracted with 25 mM HCl (250 $\mu$L) at 4°C. After centrifugation (5 min at 5,000*g* at 4°C), the supernatant was mixed with activated charcoal (7 mg) to remove pigments. Centrifugation was repeated, and 200 $\mu$L of supernatant was cleared through a glass fiber filter. For $H_2O_2$ determination, 25-$\mu$L aliquots of the extract were mixed with 445 $\mu$L of 50 mM HEPES (pH 7.5) and incubated with or without catalase (20 units) at 22°C for 1 min. Thereafter, 15 $\mu$L of 50 mM homovanillic acid in 50 mM HEPES (pH 7.5) was added, and the reaction was started by adding 15 $\mu$L of 4 $\mu$M horseradish peroxidase. After incubation at 22°C for 30 min, the relative fluorescence (excitation, 315 nm; emission, 425 nm) was measured. In parallel, a dilution series of $H_2O_2$ was measured to generate a standard curve spanning from 0 to 25 nmol of $H_2O_2$. Total $H_2O_2$ concentrations were calculated from the difference in apparent $H_2O_2$ concentrations between the noncatalase- and catalase-treated samples.

To determine the substrate specificity of 2CPA, enzymatic conversion of $H_2O_2$ and *t*-BOOH was measured using the Ferrous Oxidation-Xylenol Orange assay (Jiang et al., 1990; Nourooz-Zadeh et al., 1994). The assay was performed at 25°C and started by addition of the peroxide solution. The final reaction mixture (250 $\mu$L) contained 5 $\mu$M 2CPA, 25 $\mu$M peroxide ($H_2O_2$ or *t*-BOOH), and 100 $\mu$M DTT in 25 mM potassium phosphate buffer (pH 7.2). After different

time points (0–10 min), 10 μL of reaction mixture was added to 200 μL of Ferrous Oxidation-Xylenol Orange working reagent (250 mM sulfuric acid, 1 M sorbitol, 2.5 mM ferrous ammonium sulfate, and 1.25 mM xylenol orange in water), and the absorbance was measured spectrophotometrically at 595 nm. As negative controls, assays were performed without enzyme or with heat-inactivated enzyme (30 min at 95°C).

## Gene Expression Analysis

Total RNA was extracted from leaves using the E.Z.N.A. Plant RNA Kit (Omega Bio-Tek). Potential DNA contamination was removed using on-column digestion with DNase I. After quantification using an ND-1000 UV-Vis Spectrophotometer (NanoDrop), 1 μg of total RNA was used for complementary DNA synthesis with M-MLV RNase H Minus Reverse Transcriptase (Promega). A SYBR-Green Capillary Mix (ThermoFisher Scientific) was used for quantitative PCR with a CFX 96 Real-Time System C1000 Thermal Cycler (Bio-Rad) or a Mastercycler ep Fradient S (Eppendorf) using recommended cycle conditions. The primer pairs used are listed in Supplemental Table S1. Gene expression relative to *ACTIN2/ACTIN8* (Mueller et al., 2008) was measured by using the delta cycle threshold method (Pfaffl et al., 2004).

## Analysis of Galactolipids and Hydroperoxy Fatty Acids

For galactolipid quantification, leaves from 6-week-old plants (100 mg) were harvested, immediately shock frozen, ground in liquid nitrogen, and extracted with 500 μL of 2-propanol containing the radical scavenger butylated hydroxytoluene (4.5 mM) and (18:0, 18:0)MGDG (15 μM; internal standard). For quantification of total oxidized endogenous MGDGs (hydroperoxy- and hydroxy-MGDGs), triphenyl phosphine (TPP; 5 mg) was added to the extraction solvent to reduce hydroperoxy-MGDGs to the corresponding hydroxy-MGDGs. For determination of endogenous hydroxy-MGDGs, TPP was not included in the extraction solvent. Levels of hydroperoxy-MGDGs were calculated by subtracting the levels of hydroxy-MGDGs from the level of total oxidized MGDGs. Samples were sonicated for 5 min, incubated for 15 min on ice, and centrifuged, and the supernatant was recovered. After reextraction of the residue using the same extraction procedure, the supernatants were pooled, taken to dryness under vacuum, and reconstituted in 100 μL of 2-propanol, and 5 μL was analyzed by ultra-performance liquid-chromatography (UPLC) coupled to an electrospray ionization (ESI) hybrid quadrupole time-of-flight (qTOF) mass spectrometer (MS).

UPLC-mass spectrometry analyses were performed on an ultraperformance liquid chromatograph (Acquity UPLC; Waters) coupled to a hybrid quadrupole orthogonal time-of-flight mass spectrometer equipped with electrospray ionization source (ESI-qTOF-mass spectrometry; SYNAPT G2 HDMS; Waters). Lipids were separated on a BEH C18 Analytical Column (particle size of 1.7 μm, dimension of 2.1 × 100 mm; Waters) using a solvent gradient from 30% (v/v) to 100% (v/v) eluent B over 10 min at a temperature of 60°C and a flow rate of 0.3 mL $min^{-1}$. Eluent A consisted of 10 mM ammonium acetate in water:acetonitrile (60:40, v/v), and eluent B consisted of 10 mM ammonium acetate in 2-propanol: acetonitrile (90:10, v/v). For the detection of the analytes, negative ESI was applied using capillary voltage of 0.8 kV. The flow rate of the desolvation gas (nitrogen) was 800 L $h^{-1}$, and the desolvation temperature was kept at 350°C. MassLynx and QuantLynx software (version 4.1; Waters) were applied for data analysis (processing of chromatograms, peak detection, and integration). For determination of response factors, (18:3, 18:3)MGDG was isolated from pumpkin (*Cucurbita maxima*) leaves, and (18:3, 18:3-OH)MGDG was produced by photooxidation and TPP reduction as described (Triantaphylidès et al., 2008).

For in vitro analysis of the substrate specificity of recombinant 2CPA, 13-hydroperoxy octadecatrienoic acid (Cayman Chemicals) was quantified by UPLC-ESI-qTOF-mass spectrometry. The reversed-phase separation was performed on a BEH C18 Analytical Column (1.7 μm, 2.1 × 100 mm; Waters) using a linear solvent gradient from water:acetonitrile (30:70, v/v) to water: acetonitrile (0:100, v/v) containing 0.1% (v/v) formic acid over 10 min at 30°C. Quantification was performed by calibration using standard solutions at a concentration of 2.5 to 25 μM.

## Determination of Anthocyanins

Anthocyanin levels were determined as described (Rabino and Mancinelli, 1986). Briefly, leaves (100 mg) were harvested and shock frozen. After adding 1 mL of methanol containing 1% (v/v) HCl and 0.5 mL of water, the sample was ground with a mortar and pestle and incubated overnight at 4°C. After centrifugation at 21,000*g* for 15 min, the supernatant was collected, and the absorbances at 657 and 530 nm were measured. Anthocyanin content was calculated from the absorption at 530 nm corrected for the background absorption at 657 nm.

## Supplemental Data

The following supplemental materials are available.

**Supplemental Figure S1.** Isolation of the *2cpa 2cpb* double mutant.

**Supplemental Figure S2.** Suc sensitivity of wild-type, *2cpa*, *2cpb*, and *2cpa 2cpb* mutant plants.

**Supplemental Figure S3.** Growth phenotype and lower chlorophyll content of the *2cpa 2cpb* mutant.

**Supplemental Figure S4.** Leaf pigmentation and aromatic amino acid levels in wild-type and *2cpa 2cpb* mutant plants.

**Supplemental Figure S5.** Ascorbate, glutathione, and jasmonate levels in wild-type and *2cpa 2cpb* mutant plants.

**Supplemental Table S1.** Primers used for genotyping and quantitative gene expression analysis.

## ACKNOWLEDGMENTS

We thank Karl J. Dietz for providing *E. coli*-expressing Arabidopsis 2-Cys PRXs; Ulrich Schreiber, Ulrich Heber, and Enrique Lopéz Sanjurjo for advice concerning analysis of photosynthetic parameters; Hubert Bauer for support with gas exchange measurements; and anonymous reviewers for helpful comments.

Received December 10, 2014; accepted February 6, 2015; published February 9, 2015.

## LITERATURE CITED

**Asada K** (1999) THE WATER-WATER CYCLE IN CHLOROPLASTS: scavenging of active oxygens and dissipation of excess photons. Annu Rev Plant Physiol Plant Mol Biol **50:** 601–639

**Baier M, Noctor G, Foyer CH, Dietz KJ** (2000) Antisense suppression of 2-cysteine peroxiredoxin in Arabidopsis specifically enhances the activities and expression of enzymes associated with ascorbate metabolism but not glutathione metabolism. Plant Physiol **124:** 823–832

**Bauer H, Ache P, Lautner S, Fromm J, Hartung W, Al-Rasheid KA, Sonnewald S, Sonnewald U, Kneitz S, Lachmann N, et al** (2013) The stomatal response to reduced relative humidity requires guard cell-autonomous ABA synthesis. Curr Biol **23:** 53–57

**Birtic S, Ksas B, Genty B, Mueller MJ, Triantaphylidès C, Havaux M** (2011) Using spontaneous photon emission to image lipid oxidation patterns in plant tissues. Plant J **67:** 1103–1115

**Bonfig KB, Schreiber U, Gabler A, Roitsch T, Berger S** (2006) Infection with virulent and avirulent P. syringae strains differentially affects photosynthesis and sink metabolism in Arabidopsis leaves. Planta **225:** 1–12

**Clarke JD** (2009) Cetyltrimethyl ammonium bromide (CTAB) DNA miniprep for plant DNA isolation. Cold Spring Harb Protoc **2009:** pdb.prot5177

**Creissen G, Firmin J, Fryer M, Kular B, Leyland N, Reynolds H, Pastori G, Wellburn F, Baker N, Wellburn A, et al** (1999) Elevated glutathione biosynthetic capacity in the chloroplasts of transgenic tobacco plants paradoxically causes increased oxidative stress. Plant Cell **11:** 1277–1292

**Davletova S, Rizhsky L, Liang H, Shengqiang Z, Oliver DJ, Coutu J, Shulaev V, Schlauch K, Mittler R** (2005) Cytosolic ascorbate peroxidase 1 is a central component of the reactive oxygen gene network of *Arabidopsis*. Plant Cell **17:** 268–281

**Dietz KJ** (2011) Peroxiredoxins in plants and cyanobacteria. Antioxid Redox Signal **15:** 1129–1159

**Dietz KJ, Jacob S, Oelze ML, Laxa M, Tognetti V, de Miranda SM, Baier M, Finkemeier I** (2006) The function of peroxiredoxins in plant organelle redox metabolism. J Exp Bot **57:** 1697–1709

**Farmer EE, Mueller MJ** (2013) ROS-mediated lipid peroxidation and RES-activated signaling. Annu Rev Plant Biol **64:** 429–450

**Foyer CH, Bloom AJ, Queval G, Noctor G** (2009) Photorespiratory metabolism: genes, mutants, energetics, and redox signaling. Annu Rev Plant Biol **60:** 455–484

**Giacomelli L, Masi A, Ripoll DR, Lee MJ, van Wijk KJ** (2007) Arabidopsis thaliana deficient in two chloroplast ascorbate peroxidases shows accelerated light-induced necrosis when levels of cellular ascorbate are low. Plant Mol Biol **65:** 627–644

**Giacomelli L, Rudella A, van Wijk KJ** (2006) High light response of the thylakoid proteome in arabidopsis wild type and the ascorbate-deficient mutant *vtc2-2*. A comparative proteomics study. Plant Physiol **141:** 685–701

**Havaux M, Triantaphylidès C, Genty B** (2006) Autoluminescence imaging: a non-invasive tool for mapping oxidative stress. Trends Plant Sci **11:** 480–484

**Horling F, Lamkemeyer P, König J, Finkemeier I, Kandlbinder A, Baier M, Dietz KJ** (2003) Divergent light-, ascorbate-, and oxidative stress-dependent regulation of expression of the peroxiredoxin gene family in Arabidopsis. Plant Physiol **131:** 317–325

**Jabs T, Dietrich RA, Dangl JL** (1996) Initiation of runaway cell death in an Arabidopsis mutant by extracellular superoxide. Science **273:** 1853–1856

**Jiang ZY, Woollard AC, Wolff SP** (1990) Hydrogen peroxide production during experimental protein glycation. FEBS Lett **268:** 69–71

**Jung HS, Crisp PA, Estavillo GM, Cole B, Hong F, Mockler TC, Pogson BJ, Chory J** (2013) Subset of heat-shock transcription factors required for the early response of Arabidopsis to excess light. Proc Natl Acad Sci USA **110:** 14474–14479

**Kangasjärvi S, Lepistö A, Hännikäinen K, Piippo M, Luomala EM, Aro EM, Rintamäki E** (2008) Diverse roles for chloroplast stromal and thylakoid-bound ascorbate peroxidases in plant stress responses. Biochem J **412:** 275–285

**Kangasjärvi S, Neukermans J, Li S, Aro EM, Noctor G** (2012) Photosynthesis, photorespiration, and light signalling in defence responses. J Exp Bot **63:** 1619–1636

**Kitajima S** (2008) Hydrogen peroxide-mediated inactivation of two chloroplastic peroxidases, ascorbate peroxidase and 2-cys peroxiredoxin. Photochem Photobiol **84:** 1404–1409

**König J, Baier M, Horling F, Kahmann U, Harris G, Schürmann P, Dietz KJ** (2002) The plant-specific function of 2-Cys peroxiredoxin-mediated detoxification of peroxides in the redox-hierarchy of photosynthetic electron flux. Proc Natl Acad Sci USA **99:** 5738–5743

**König J, Galliardt H, Jütte P, Schäper S, Dittmann L, Dietz KJ** (2013) The conformational bases for the two functionalities of 2-cysteine peroxiredoxins as peroxidase and chaperone. J Exp Bot **64:** 3483–3497

**Lehtimäki N, Shunmugam S, Jokela J, Wahlsten M, Carmel D, Keränen M, Sivonen K, Aro EM, Allahverdiyeva Y, Mulo P** (2011) Nodularin uptake and induction of oxidative stress in spinach (Spinachia oleracea). J Plant Physiol **168:** 594–600

**Maruta T, Tanouchi A, Tamoi M, Yabuta Y, Yoshimura K, Ishikawa T, Shigeoka S** (2010) Arabidopsis chloroplastic ascorbate peroxidase isoenzymes play a dual role in photoprotection and gene regulation under photooxidative stress. Plant Cell Physiol **51:** 190–200

**Miyake C** (2010) Alternative electron flows (water-water cycle and cyclic electron flow around PSI) in photosynthesis: molecular mechanisms and physiological functions. Plant Cell Physiol **51:** 1951–1963

**Mueller S, Hilbert B, Dueckershoff K, Roitsch T, Krischke M, Mueller MJ, Berger S** (2008) General detoxification and stress responses are mediated by oxidized lipids through TGA transcription factors in *Arabidopsis*. Plant Cell **20:** 768–785

**Nguyen D** (2013) Quantifying chromogen intensity in immunohistochemistry via reciprocal intensity. Protoc exch doi:10.1038/protex.2013.097

**Nourooz-Zadeh J, Tajaddini-Sarmadi J, Wolff SP** (1994) Measurement of plasma hydroperoxide concentrations by the ferrous oxidation-xylenol orange assay in conjunction with triphenylphosphine. Anal Biochem **220:** 403–409

**Page M, Sultana N, Paszkiewicz K, Florance H, Smirnoff N** (2012) The influence of ascorbate on anthocyanin accumulation during high light acclimation in Arabidopsis thaliana: further evidence for redox control of anthocyanin synthesis. Plant Cell Environ **35:** 388–404

**Pfaffl MW, Tichopad A, Prgomet C, Neuvians TP** (2004) Determination of stable housekeeping genes, differentially regulated target genes and sample integrity: BestKeeper—Excel-based tool using pair-wise correlations. Biotechnol Lett **26:** 509–515

**Puerto-Galán L, Pérez-Ruiz JM, Ferrández J, Cano B, Naranjo B, Nájera VA, González M, Lindahl AM, Cejudo FJ** (2013) Overoxidation of chloroplast 2-Cys peroxiredoxins: balancing toxic and signaling activities of hydrogen peroxide. Front Plant Sci **4:** 310

**Pulido P, Spínola MC, Kirchsteiger K, Guinea M, Pascual MB, Sahrawy M, Sandalio LM, Dietz KJ, González M, Cejudo FJ** (2010) Functional analysis of the pathways for 2-Cys peroxiredoxin reduction in Arabidopsis thaliana chloroplasts. J Exp Bot **61:** 4043–4054

**Queval G, Issakidis-Bourguet E, Hoeberichts FA, Vandorpe M, Gakière B, Vanacker H, Miginiac-Maslow M, Van Breusegem F, Noctor G** (2007) Conditional oxidative stress responses in the Arabidopsis photorespiratory mutant cat2 demonstrate that redox state is a key modulator of daylength-dependent gene expression, and define photoperiod as a crucial factor in the regulation of H2O2-induced cell death. Plant J **52:** 640–657

**Rabino I, Mancinelli AL** (1986) Light, temperature, and anthocyanin production. Plant Physiol **81:** 922–924

**Rizhsky L, Liang H, Mittler R** (2003) The water-water cycle is essential for chloroplast protection in the absence of stress. J Biol Chem **278:** 38921–38925

**Rouhier N, Jacquot JP** (2002) Plant peroxiredoxins: alternative hydroperoxide scavenging enzymes. Photosynth Res **74:** 259–268

**Schreiber U** (2004) Pulse-amplitude-Modulation (PAM) fluorometry and saturation pulse method: an overview. *In* GC Papageorgiou, Govinjee, eds, Chlorophyll a fluorescence: A signature of photosynthesis. Springer, Dordrecht, The Netherlands, pp 279–319

**Shan X, Zhang Y, Peng W, Wang Z, Xie D** (2009) Molecular mechanism for jasmonate-induction of anthocyanin accumulation in Arabidopsis. J Exp Bot **60:** 3849–3860

**Shigeoka S, Ishikawa T, Tamoi M, Miyagawa Y, Takeda T, Yabuta Y, Yoshimura K** (2002) Regulation and function of ascorbate peroxidase isoenzymes. J Exp Bot **53:** 1305–1319

**Spector T** (1978) Refinement of the coomassie blue method of protein quantitation. A simple and linear spectrophotometric assay for less than or equal to 0.5 to 50 microgram of protein. Anal Biochem **86:** 142–146

**Suzuki YJ, Carini M, Butterfield DA** (2010) Protein carbonylation. Antioxid Redox Signal **12:** 323–325

**Triantaphylidès C, Krischke M, Hoeberichts FA, Ksas B, Gresser G, Havaux M, Van Breusegem F, Mueller MJ** (2008) Singlet oxygen is the major reactive oxygen species involved in photooxidative damage to plants. Plant Physiol **148:** 960–968

**van Kooten O, Snel JF** (1990) The use of chlorophyll fluorescence nomenclature in plant stress physiology. Photosynth Res **25:** 147–150

**Vandenabeele S, Vanderauwera S, Vuylsteke M, Rombauts S, Langebartels C, Seidlitz HK, Zabeau M, Van Montagu M, Inzé D, Van Breusegem F** (2004) Catalase deficiency drastically affects gene expression induced by high light in Arabidopsis thaliana. Plant J **39:** 45–58

**Vanderauwera S, Zimmermann P, Rombauts S, Vandenabeele S, Langebartels C, Gruissem W, Inzé D, Van Breusegem F** (2005) Genome-wide analysis of hydrogen peroxide-regulated gene expression in Arabidopsis reveals a high light-induced transcriptional cluster involved in anthocyanin biosynthesis. Plant Physiol **139:** 806–821

**Wood ZA, Poole LB, Karplus PA** (2003) Peroxiredoxin evolution and the regulation of hydrogen peroxide signaling. Science **300:** 650–653

**Zoeller M, Stingl N, Krischke M, Fekete A, Waller F, Berger S, Mueller MJ** (2012) Lipid profiling of the Arabidopsis hypersensitive response reveals specific lipid peroxidation and fragmentation processes: biogenesis of pimelic and azelaic acid. Plant Physiol **160:** 365–378